SIMS proceedings paper

SURFACE and INTERFACE ANALYSIS

Received: 29 September 2011 Revised: 19 December 2011 Accepted: 2 February 2012 Published online in Wiley Online Library: 1 March 2012

(wileyonlinelibrary.com) DOI 10.1002/sia.4905

Modeling dynamic cluster SIMS experiments

Barbara J. Garrison,[a]* Zachary J. Schiffer,[a] Paul E. Kennedy[a] and Zbigniew Postawa[b]

The underpinnings of two SIMS experimental findings are elucidated using the power of molecular dynamics to provide insight at the molecular level. First, the improvement of depth resolution for C_{60} bombardment of Irganox delta layers and polymer layers using sample rotation is explained by molecular dynamics simulations of the repetitive bombardment of Ag surfaces with 20 keV Au_3, C_{60}, and Ar_{872} at grazing angles of incidence with both single azimuthal angle and random azimuthal angles. Single azimuthal angle simulations at grazing angles show the formation of trenches and valleys parallel to the cluster beam form and are elongated with increasing incident angle. Cluster bombardment simulations with random azimuthal angles mimic sample rotation and show that under grazing angles of incidence, the surface is smoother because of the random impact angles preventing trench and valley formation. Second, depth profiles using C_{60} at a 70° angle of incidence have been improved by co-bombardment with low energy Ar ions emitted at 33° from the C_{60} beam and at a 45° incident angle from the surface. Molecular dynamics simulations of the bombardment of solid benzene with low energy Ar and 15 keV C_{60} were used to show the depth of damage created during bombardment. For low kinetic energy (<200 eV), the damage caused by the Ar atom is in the same region as for the C_{60} cluster. It is believed that for the experimental conditions used during co-bombardment, the Ar beam is breaking up the ridges created by the grazing C_{60} beam. Copyright © 2012 John Wiley & Sons, Ltd.

Keywords: SIMS; molecular dynamics; sample rotation; co-bombardment; depth profile; C_{60}; Ar

Introduction

Molecular dynamics (MD) simulations have been a partner to SIMS experiments over the decades.[1] As the experiments move toward depth profiling with cluster beams, the computational challenges increase. Here we discuss two examples of where MD simulations are used to interpret experimental results. In the first example, repetitive bombardment simulations using the divide and conquer protocol[2] are implemented to explain the effect of sample rotation on depth profiling.[3] In this case, the comparison between simulation and experimental results is relatively straightforward, and the MD simulations provide a mechanistic insight as to why sample rotation should work. In the second example, we examine the effect of low energy Ar co-bombardment as a means of improving C_{60} depth profiles.[4,5] In this case, the interpretation is more intricate, weaving together a logical explanation based on the simulations and the experimental data.

Repetitive bombardment simulations—understanding the effect of sample rotation on depth profiling

The experimental observation of interest here is that rotation of the sample during erosion improves the depth resolution for C_{60} bombardment of Irganox delta layers[3] as well as polymer layers. Calculations aimed at explaining this observation were performed for C_{60} bombardment of Ag at 20 keV at 45° and 70° incidence at a single azimuthal angle of incidence and for random azimuthal angles of incidence, a computational approach for sample rotation.[6]

The calculated RMS roughness values for the five calculations are shown in Table 1.[6] The RMS roughness decreases with increasing incident angle. Using a random incident angle, the computational equivalent of sample rotation, reduces the RMS roughness for primarily the 70° incidence.

A visual inspection of the surfaces with single and random impact directions shows that there are trenches and valleys parallel to the beam for the single azimuth simulation and that the peaks and valleys are more extended than for the random azimuth simulations as shown in Fig. 1. To quantitate the differences, an additional measure of the surface topography is used for a wider range of cluster projectiles. The lateral anisotropy is shown in Fig. 2 and is represented as the number of times that the sample height crosses the mean surface level per 1 nm length in each row or column of the sampling grid. For the simulations with a single azimuthal direction, the number of crossings in the direction perpendicular to the beam (*y*-direction) is greater than that in the direction parallel to the beam (*x*-direction) as shown in Figs. 2a–2c for 70° incidence of 20 keV Au_3, C_{60}, and Ar_{872}, respectively. This confirms the visual observation that trenches and ridges are formed parallel to the beam direction for a single incident azimuthal direction.[6] The effect is the most pronounced for Ar_{872}. For the random azimuthal angle simulations, the number of crossings in each direction is the same as

* *Correspondence to: Barbara J. Garrison, Department of Chemistry, Penn State University, 104 Chemistry Building, University Park, PA 16802, USA. E-mail: bjg@psu.edu*

a *Department of Chemistry, Penn State University, University Park, PA 16802, USA*

b *Smoluchowski Institute of Physics, Jagiellonian University, ul. Reymonta 4, 30-059 Kraków, Poland*

Table 1. RMS roughness induced by 20 keV C_{60} projectile at various bombardment conditions

Projectile	RMS roughness (nm)
20 keV C_{60} 0°	2.4
20 keV C_{60} 45°	2.1
20 keV C_{60} 45° random azimuth	1.9
20 keV C_{60} 70°	1.3
20 keV C_{60} 70° random azimuth	1.0

The maximum difference in RMS roughness value from the mean value for 0° and 45° is ±0.1 nm and for 70° is ±0.06 nm.

seen in Fig. 2d for 20 keV C_{60}. Clearly, the effect of sample rotation or random azimuthal direction of incidence is to make the surface smoother by preventing the buildup of the large elongated ridges and valleys on the sample. Impacts parallel to the ridge tend to enhance the ridge, whereas impacts perpendicular to the ridge tend to break it down. Zalar proposed sample rotation during atomic bombardment for depth profiling with XPS[7] as a means to even out sputtering yields due to heterogeneities of the sample.[8] As indicated by results for C_{60} bombardment, the sample rotation obliterates anisotropy developed by the impinging beam at grazing incidence. However, the process is efficient only at grazing incidence angle. On the basis of calculations for a single angle of incidence, we predict that sample rotation at 70° will also help experiments using Au_3 and large Ar cluster beams.[6]

C_{60} and low energy Ar co-bombardment

An intriguing set of experiments from Shyue *et al.*[4,5,9–15] shows promise of assisting depth profiles by co-bombardment of the system with C_{60} and low energy Ar ions. This strategy for eroding samples has, as yet, only been implemented by one research group because most SIMS instruments with C_{60} ion beams do not also have a low energy Ar ion beam. We have performed MD computer simulations that provide insight into the interplay of effects in the solid by C_{60} co-bombardment with low energy Ar ions.

A general schematic of the experimental configuration is shown in Fig. 3. Both beams are incident on the surface with the Ar beam having approximately 30 times the dose as the C_{60} beam. Full simulations of depth profiling with the dual beams are not tractable at this time, thus we looked at the effects of each beam individually on a generic benzene crystal.[16] To understand the relationship between Ar and C_{60}, simulations of both Ar and C_{60} bombardment were performed. Argon atoms with 100, 200, 300, and 400 eV incidence energies were used to bombard benzene solids at an incident polar angle of 45°. Fifty trajectories were run at each incident energy. Simulations were performed for 15 keV C_{60} bombardment using a combined atomistic and coarse-grained representation as presented elsewhere in this volume.[17]

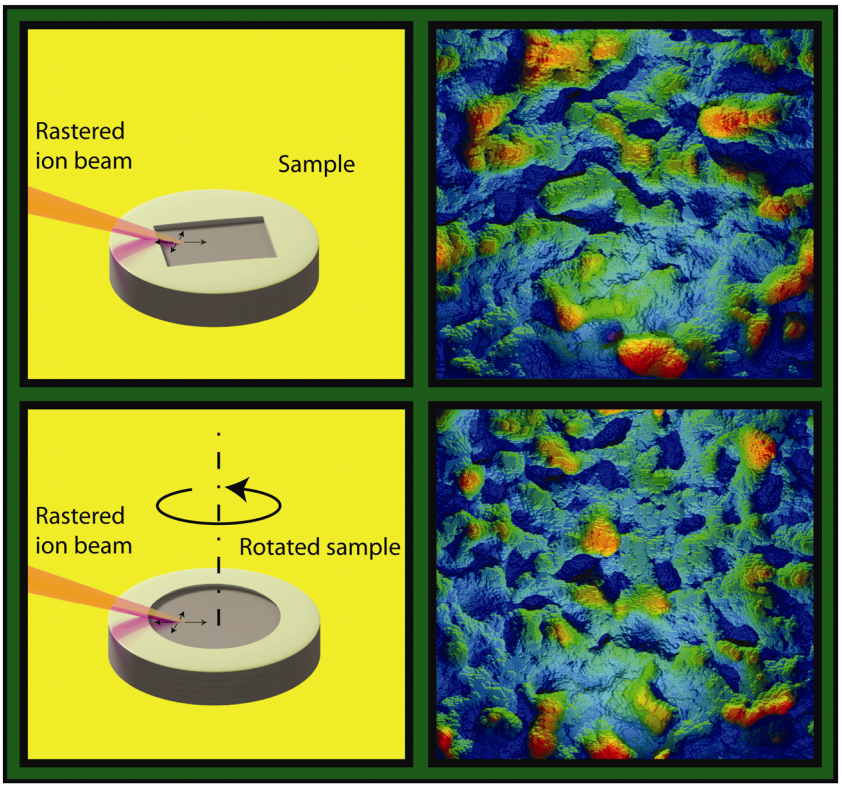

Figure 1. Schematic of single and random azimuthal angle bombardment along with the roughened surface. The lighter colors are higher elevation and the darker colors are lower elevation. Reprinted from *Chem. Phys. Lett.*, 506, Barbara J. Garrison and Zbigniew Postawa, "Effect of sample rotation on surface roughness with keV C_{60} bombardment in secondary ion mass spectrometry (SIMS) experiments," 129–134, 2011, with permission from Elsevier.

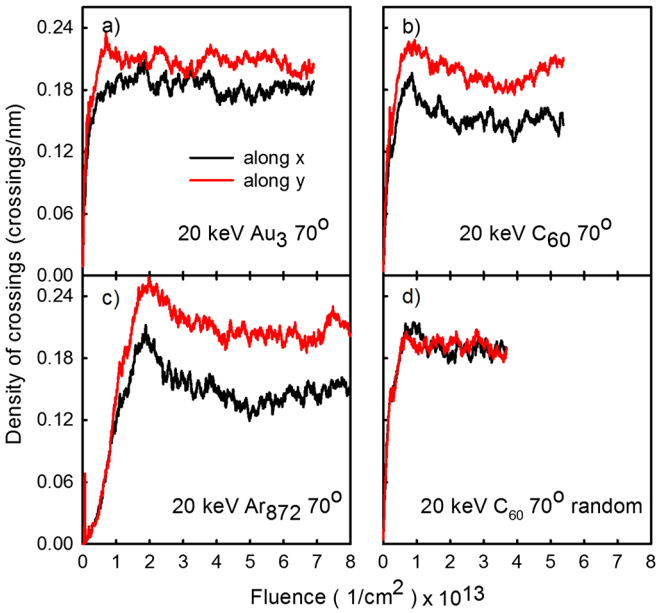

Figure 2. The number of crossings per nanometer in the direction perpendicular to the beam (*y*-direction; gray line) and parallel to the beam (*x*-direction; black line) as a function of fluence. (a) The 20-keV 70° polar incident angle Au_3, single azimuth. (b) The 20-keV 70° polar incident angle C_{60}, single azimuth. (c) The 20-keV 70° polar incident angle Ar_{872}, single azimuth. (d) The 20 keV 70° polar incident angle C_{60}, random azimuth.

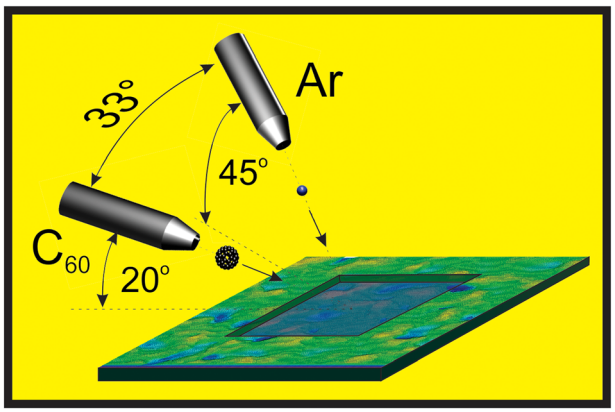

Figure 3. Schematic of the C_{60} and Ar co-bombardment arrangement.

There are several possible reasons that may account for better depth profiling in co-sputtering experiments. First, as predicted by an erosion dynamics model, the total sputtering yield relative to the damage created should be large for effective depth profiling.[18] The experimental sputtering yield reported by You *et al.*[4] ranges from 1 to 3 nm^3 per incident ion. This yield is, however, very small compared with, for example, the experimental yield for 40 keV C_{60} bombardment of cholesterol at 73° incident angle, for which the yield is two orders of magnitude larger.[19] The simulations clearly show the yield from the Ar sputtering is miniscule compared with C_{60}; thus, the Ar is not contributing significantly to the sputtering yield.

There is another possibility that may contribute to the enhancement of the depth profiles[4,5] of organic solids with co-bombardment by C_{60} and 200 eV Ar when compared with C_{60} bombardment. As discussed earlier, high-fluence simulations of C_{60} impacts show that C_{60} bombardment at 70° incidence creates a roughened surface with elongated ridges and valleys parallel to the beam direction. Computer simulations show that by using sample rotation, these elongated ridges and valleys do not form, the surface gets smoother, and the sputtering yield increases by approximately 10%. This value is actually comparable with the yield increase with co-sputtering reported by You *et al.*[4] for organic, polymeric samples. Thus, we propose that the Ar beam, which is oriented 33° with respect to the C_{60} beam, is breaking up the ridges formed by the C_{60} bombardment, effectively smoothing the surface. The key aspect of the low (<200 eV) kinetic energy of the incident Ar projectiles is that the damage induced by these projectiles is kept in the same region as damage created by the C_{60} bombardment. A graphical depiction of this information is presented schematically in Fig. 4a where a 5-nm slice of the crater region for C_{60} bombardment is shown. The red molecules are damaged molecules. Also shown is damage associated with trajectories that exhibit an average number of damaged molecules for 200 and 300 eV Ar bombardment. Clearly, the 200-eV Ar bombardment confines its damage to the altered layer of the C_{60} bombardment, whereas the 300-eV Ar bombardment extends the damage into pristine sample. Taking into account this explanation for the enhancement due to co-bombardment by the cluster and atomic projectiles, we would not expect this synergy to exist for angles of incidence closer to the surface normal nor would we expect the enhancement for C_{60} beam conditions that give much higher yields. A change

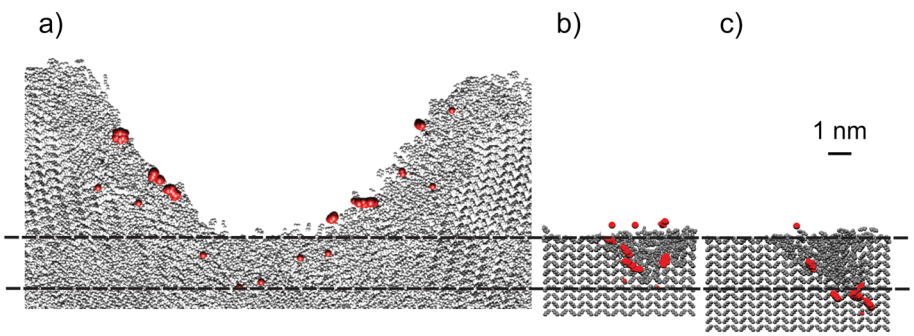

Figure 4. Location of the molecular fragments (red and enlarged) created by (a) 15 keV C_{60} bombardment of solid benzene at a normal incidence and (b) 200 and (c) 300 eV Ar at 45° impact angle. The trajectories are selected to represent average damage. Only the molecules located in a slice 5-nm wide, centered at the point of projectile impact, are shown. In addition, for nondamaged molecules, only the C atoms are shown. The snapshots are aligned so that the surfaces of Ar bombarded samples correspond to the bottom of the crater induced by C_{60} impact to easily compare the damage induced by these two projectiles. Reprinted with permission from Schiffer, Z. J.; Kennedy, P. E.; Postawa, Z.; Garrison, B. J. Molecular Dynamics Simulations Elucidate the Synergy of C_{60} and Low Energy Ar Co-bombardment for Molecular Depth Profiling. Journal of Physical Chemistry Letters 2011, 2, 2635-2638. Copyright (2011) American Chemical Society.

SURFACE and INTERFACE ANALYSIS

in the C_{60} conditions might be just as effective in improving the depth profile as co-bombardment with low energy Ar ions.

Conclusion

We have presented two examples in which MD computer simulations provide direct interpretation of experimental SIMS results. First, we give mechanistic insight into why sample rotation works for grazing angles of incidence. Second, we explain the effect of co-bombardment of C_{60} with low energy Ar.

Acknowledgements

The authors gratefully acknowledge financial support from the National Science Foundation (grant no. CHE-0910564) and the Polish Ministry of Science and Higher Education (program no. PB1839/B/H03/2011/40). Computational resources were provided by the Research Computing and Cyberinfrastructure group at Penn State University.

References

[1] B. J. Garrison, Z. Postawa, *Mass Spectrom. Rev.* **2008**, *27*, 289.
[2] M. F. Russo, Z. Postawa, B. J. Garrison, *J. Phys. Chem. C* **2009**, *113*, 3270.
[3] P. Sjovall, D. Rading, S. Ray, L. Yang, A. G. Shard, *J. Phys. Chem. B* **2010**, *114*, 769.
[4] Y. W. You, H. Y. Chang, W. C. Lin, S. H. Lee, W. L. Kao, G. J. Yen, C. J. Chang, C. P. Liu, C. C. Huang, H. Y. Liao, J. J. Shyue, *Rapid Commun. Mass Spectrom.* **2011**, *25*(19), 2897–2904.
[5] B. Y. Yu, Y. Y. Chen, W. B. Wang, M. F. Hsu, S. P. Tsai, W. C. Lin, Y. C. Lin, J. H. Jou, C. W. Chu, J. J. Shyue, *Anal. Chem.* **2008**, *80*, 3412.
[6] B. J. Garrison, Z. Postawa, *Chem. Phys. Lett.* **2011**, *506*, 129.
[7] A. Zalar, *Thin Solid Films* **1985**, *124*, 223.
[8] M. P. Seah, C. Lea, *Thin Solid Films* **1981**, *81*, 257.
[9] W. C. Lin, Y. C. Lin, W. B. Wang, B. Y. Yu, S. Iida, M. Tozu, M. F. Hsu, J. H. Jou, J. J. Shyue, *Org. Electron.* **2009**, *10*, 459.
[10] W. C. Lin, C. P. Liu, C. H. Kuo, H. Y. Chang, C. J. Chang, T. H. Hsieh, S. H. Lee, Y. W. You, W. L. Kao, G. J. Yen, C. C. Huang, J. J. Shyue, *Analyst* **2011**, *136*, 941.
[11] W. C. Lin, W. B. Wang, Y. C. Lin, B. Y. Yu, Y. Y. Chen, M. F. Hsu, J. H. Jou, J. J. Shyue, *Org. Electron.* **2009**, *10*, 581.
[12] Y. C. Lin, Y. Y. Chen, B. Y. Yu, W. C. Lin, C. H. Kuo, J. J. Shyue, *Analyst* **2009**, *134*, 945.
[13] B. Y. Yu, W. C. Lin, Y. Y. Chen, Y. C. Lin, K. T. Wong, J. J. Shyue, *Appl. Surf. Sci.* **2008**, *255*, 2490.
[14] B. Y. Yu, W. C. Lin, J. H. Huang, C. W. Chu, Y. C. Lin, C. H. Kuo, S. H. Lee, K. T. Wong, K. C. Ho, J. J. Shyue, *Anal. Chem.* **2009**, *81*, 8936.
[15] B. Y. Yu, C. Y. Liu, W. C. Lin, W. B. Wang, I. M. Lai, S. Z. Chen, S. H. Lee, C. H. Kuo, W. L. Kao, Y. W. You, C. P. Liu, H. Y. Chang, J. H. Jou, J. J. Shyue, *ACS Nano* **2010**, *4*, 2547.
[16] Z. J. Schiffer, P. E. Kennedy, Z. Postawa, B. J. Garrison, *J. Phys. Chem. Lett.* **2011**, *2*, 2635–2638.
[17] P. Kennedy, B. J. Garrison, *Surf. Interface Anal.*, to be submitted.
[18] J. Cheng, A. Wucher, N. Winograd, *J. Phys. Chem. B* **2006**, *110*, 8329.
[19] J. Kozole, A. Wucher, N. Winograd, *Anal. Chem.* **2008**, *80*, 5293.

